

# A feedback SIR (fSIR) model highlights advantages and limitations of infection-based social distancing

Elisa Franco,  
Department of Mechanical and Aerospace Engineering,  
Department of Bioengineering,  
University of California, Los Angeles

## ABSTRACT

Transmission rates in epidemic outbreaks vary over time depending on the societal and government response to infections and mortality data, as evidenced in the course of the COVID-19 pandemic. Following a mean field approach that models individuals like molecules in a well-mixed solution, I derive a modified SIR model in which the average daily contacts between susceptible and infected population are reduced based on the known infection levels, capturing the effects of social distancing policies. This approach yields a time-varying reproduction number that is continuously adjusted based on infection information through a negative-feedback term that is equivalent to Holling type II functions in ecology and Hill functions in chemistry and molecular biology. This feedback-adjustment of the transmission rate causes a structural reduction in infection peak, and simulations indicate that such reduction persists even in the presence of information delays. Simulations also show that a distancing policy based on infection data may substantially extend the duration of an epidemic. If the distancing rate is linearly proportional to infections, this model adds a *single* parameter to the original SIR, making it useful to illustrate the effects of social distancing enforced based on awareness of infections.

## AUTHOR SUMMARY

Is it possible to control epidemic outbreaks using current infection information? This is an important question for epidemiologists and policymakers during the COVID-19 pandemic, because daily testing data is rapidly available to the public for analysis and decision making. This manuscript provides a simple model to illustrate the effects of feedback of social distancing based on infection information. The model is derived from first principles, and where it lacks the complexity needed for accurate forecasting, it clearly highlights the tradeoffs of flattening the curve while limiting the duration of an epidemic.

## INTRODUCTION

Compartment models are the simplest approach to modeling epidemic outbreaks. Like mean-field models in physics and chemistry governed by the law of mass action, compartment models assume a well-mixed population in which individuals have average interaction and recovery patterns. The population is binned in categories, and at a minimum include those susceptible to disease (S), those who become infected (I), and those who recover and/or die (R), which are included in the well-known SIR model by Kermack and McKendrick [16]. Because the SIR model is not suited to capture epidemics with a long incubation time, a large population of asymptomatic individuals, and high lethality, many SIR variants with additional compartments have been developed and tailored to model specific epidemic outbreaks [4], [11].

Many SIR-type models include nonlinear transmission functions that capture societal responses to knowledge of infections and deaths, and are often referred to as “behavioral functions” [20], [22], [6]. For example, Bootsma and Ferguson included a nonlinear term to capture the effects of awareness of *deaths* (rather than infections) on social interactions within the 1918 influenza epidemic in the United States [4]. The reduction of transmission and contact rates achieved by infection awareness programs has been evaluated within SIS, SIR, and SEIRS models [12], [25], [26]. Models including infection awareness have also taken into account its effects on the susceptible fraction of the population [18], [10], in particular by increasing vaccination rates [5].

In the context of the COVID-19 pandemic, using infection information to regulate social distancing and thereby the transmission rates is a mechanism for individuals and policymakers to *control the course of the pandemic as it unfolds*, thanks to the improvements in widespread testing, social connectivity, and rapid access to media and news reports [8], [24], [23]. Many new modeling studies are being reported on a daily basis with recommendations for suppression and mitigation of infections, based on *open loop* (select a social distancing

protocol that discounts or ignores epidemic data) [3] or *closed loop* strategies (regulate social distancing based on collected epidemic data) [7].

In this manuscript I provide a simple derivation of a nonlinear transmission rate in which distancing based on infection awareness reduces average daily contacts. Through a timescale separation argument, I obtain a transmission rate that is equivalent to Hollinger type II and Michaelis-Menten functions. Because this transmission function depends on infection levels generating a negative feedback loop, I will refer to this model as feedback SIR (fSIR). Through mathematical analysis I show that this infection-dependent nonlinear transmission rate structurally reduces the peak of infections. If distancing depends on infections through a linear policy, the peak is also structurally postponed. With simulations, I illustrate that peak mitigation persists even in the presence of delay in the transmission of infection information, and that the corresponding delay in the peak is moderate; finally, the duration of the epidemic, measured as the time for which infections persist, may significantly increase. I also highlight that the fSIR model can qualitatively capture historical infection data for the COVID-19 pandemic.

In the special case in which the distancing mechanism is a linear function of infections, the fSIR models the societal response to epidemic information with only one parameter in addition to the reproduction number. Thus, the fSIR may be helpful as an illustrative yet rigorous model to examine alternative scenarios for epidemic spread, depending on the strictness of social distancing. Further, this model supports social distancing guidelines as it clearly shows that the infection curve can be flattened without postponing the peak, a misleading (and demotivating) scenario suggested by illustrative models that use a constant transmission rate. At the same time, the model highlights that policies relying exclusively on infection data to regulate social distancing can majorly extend the time required to reach a disease-free equilibrium.

#### A. Background: qualitative analysis of the non-dimensional SIR model

The SIR model is the simplest compartment model that can qualitatively capture the evolution of an epidemic at the population level. The model assumes well-mixed population that remains constant (without birth and death processes) and has two key parameters: 1) the transmission coefficient  $\beta$ , which depends on the social interactions among individuals (average daily contacts) and on the viral infection characteristics; the transmission rate is generally thought as the product of the average frequency of contacts between infected and susceptible and the likelihood that infection occurs given

a contact;

2) the recovery coefficient  $\gamma$ , which captures the average time for recovery (or death) of infected individuals. The inverse  $1/\gamma$  is also known as duration of infectiousness. Assuming the total population is  $N$ , the original SIR model is:

$$\frac{dS}{dt} = -\beta \frac{S}{N} I, \quad (1)$$

$$\frac{dI}{dt} = \beta \frac{S}{N} I - \gamma I, \quad (2)$$

$$\frac{dR}{dt} = \gamma I. \quad (3)$$

Because  $r = N - i - s$ , the model can be reduced to two ODEs. Further, the variables can be normalized by the total population setting  $s = S/N$ ,  $i = I/N$  (and  $r = R/N$ ); by rescaling time as  $\tau = t\gamma$ , the SIR model becomes non-dimensional, with a single coefficient  $\mathcal{R}_0 = \beta/\gamma$ , the well known reproduction ratio or reproduction number [2].

$$\frac{ds}{d\tau} = -\mathcal{R}_0 si, \quad (4)$$

$$\frac{di}{d\tau} = (\mathcal{R}_0 s - 1)i. \quad (5)$$

It is well-known that the solutions are positive and satisfy the conservation law  $s + i + r = 1$  [14], and exact expressions have been computed [13]. If there are no infected individuals ( $i_0 = 0$ ), the system remains in the infection-free equilibrium  $E_0 = (s_0, 0, 0)$  because all derivatives are identically zero. For any initial value of infections  $i_0 > 0$ , the solutions  $s(t)$  and  $i(t)$  are bounded and evolve in the invariant set  $\mathcal{P} = \{s \leq s_0, i \leq 1, r \leq 1\}$ . This follows from the fact that  $ds/d\tau \leq 0$ , so  $s(\tau) \leq s_0, \forall \tau \geq \tau_0$ . The solutions and the admissible equilibria depend on the value of  $\mathcal{R}_0$  and on the initial value of the susceptible population  $s_0$ .

If  $\mathcal{R}_0 s_0 < 1$ , the infected population is non-increasing because  $di/d\tau \leq 0$ , thus the epidemic does not start (the system reaches an infection-free equilibrium  $\bar{E} = (\bar{s}, 0, \bar{r})$ ).

If  $\mathcal{R}_0 s_0 > 1$ , then  $di/d\tau$  initially increases, reaches a peak when  $s = s_{crit} = 1/\mathcal{R}_0 \leq s_0$ , and finally decreases to zero. The equilibrium in this case is  $E = (\bar{s}, 0, \bar{r})$  (endemic equilibrium). Because  $s_0 \leq 1$ ,  $\mathcal{R}_0 s_0 > 1 \Rightarrow \mathcal{R}_0 > 1$ . For any positive  $i_0$  and  $\mathcal{R}_0 s_0 > 1$ , the relation between susceptible and infected can be computed exactly from the ratio of  $di/d\tau$  and  $ds/d\tau$  (directional derivative) [14]:

$$\frac{di}{ds} = \frac{\mathcal{R}_0 s - 1}{-\mathcal{R}_0 s} = -1 + \frac{1}{\mathcal{R}_0 s} \Rightarrow di = -ds + \frac{ds}{\mathcal{R}_0 s}.$$

Integrating we obtain the relation between  $i(\tau)$  and  $s(\tau)$ :

$$i(\tau) = i_0 + s_0 - s(\tau) - \frac{1}{\mathcal{R}_0} \log \frac{s_0}{s(\tau)}. \quad (6)$$

The peak of infections occurs when  $s = s^* = 1/\mathcal{R}_0$  ( $s = s^*$  yields  $di/d\tau = 0$ ). Substituting  $s^*$  we find:

$$i_{max} = i_0 + s_0 - \frac{1}{\mathcal{R}_0} (1 + \log(s_0 \mathcal{R}_0)), \quad (7)$$

with  $\log(s_0 \mathcal{R}_0) > 0$  because  $s_0 \mathcal{R}_0 > 1$ . From expression (6), by setting  $\bar{i} = 0$ , we can also derive an implicit equation to find the equilibrium value of the recovered population:

$$\log \frac{s_0}{\bar{s}} = \mathcal{R}_0(1 - \bar{s}),$$

which has one positive root (because  $\bar{s} < s_0 \leq 1$  and  $\mathcal{R}_0 > 1$ ). In other words, the equilibrium susceptible population is positive (not all the population has become infected), unless  $\mathcal{R}_0$  is unrealistically large.

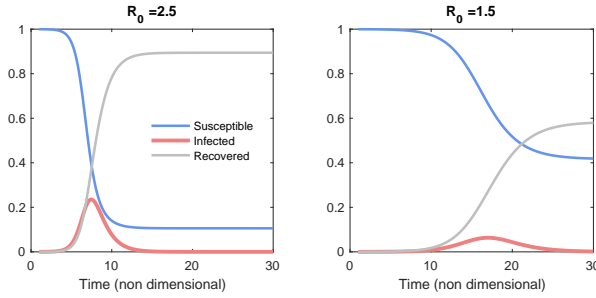


Fig. 1. Illustrative numerical simulations showing the SIR dynamics for different values of (constant) transmission rate  $\beta$ . The right plot illustrates how a lower value of  $\beta$  “flattens the curve” while also significantly delaying the infection peak. This illustration may be misleading to the public because the introduction of social distancing causes the transmission rate  $\beta$  to vary in time. Further, this picture suggests that social distancing measures may have to be imposed for a very long time to be effective, but with a time-varying  $\beta$  this may not be necessary. This manuscript describes an SIR model in which distancing depends on the (known) infection levels, introducing feedback that changes the reproduction number as a function of time.

### B. Flattening the curve: a low reproduction number reduces and delays the infection peak

The SIR model has been used to illustrate how a low reproduction number  $\mathcal{R}_0$  (or a low transmission rate  $\beta$ ) has the effect of “flattening the (infection) curve”, *i.e.* reducing the infection peak while lengthening the duration of the epidemic. The simulations in Fig. 1 compare the SIR solutions for values of  $\mathcal{R}_0 = 2.5$ , which is close to recent estimates for the COVID-19 outbreak [21], and  $\mathcal{R}_0 = 1.5$ . The infection peak is clearly reduced when  $\mathcal{R}_0 = 1.5$ , however the infection peak is also significantly delayed.

The problem with assuming a low, constant reproduction number  $\mathcal{R}_0$  is that it is misleading to the public and to policymakers. A time-dependent reproduction number  $\mathcal{R}(\tau)$  captures better a societal response in which disease awareness, social habits, and government policies may fluctuate over time. During the COVID-19 epidemic,

enormous research efforts are dedicated to a continuous estimation and forecasting of the reproduction number as a function of social distancing measures [2], [19]. Here I report the derivation of a simple candidate model for  $\mathcal{R}(\tau)$  that is based on a mean field model of social distancing, and may be helpful for illustrative purposes, to compare alternative scenarios of collective response, or to model and compare regional epidemic data.

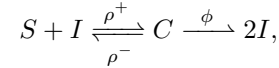
## RESULTS

### The feedback SIR (fSIR) model

Social distancing policies suggested or officially imposed by government agencies typically depend on the reported infections or deaths. With fast spread of information about testing results [8], [24], [23], knowledge of *infections* may be more helpful than deaths in quickly containing epidemics (the average time to death for COVID-19 patients, for example, is 17 days [27], which means average lethality information of an epidemic may be available with a significant delay).

Nonlinear transmission rates taking into account infection awareness have been widely described in the literature [6], [20], [22]: here we follow a derivation based on first principles using the law of mass action in chemistry, by modeling individuals and their interactions like molecules in a well-mixed solution.

A contagion may occur when a susceptible individual ( $S$ ) and an infected individual ( $I$ ) are in spatial proximity for some time (associated or contact state  $C$ ); this encounter may then result in two infected individuals. This can be modeled using the equivalent reactions:



where  $\rho^+$  and  $\rho^-$  are the rates of association and dissociation of a susceptible and an infected individual, and we can associate  $\phi$  with the probability that infection occurs. The law of mass action yields an ODE for the level of individuals in the associated state  $C$  (the ODE is written in terms of non-dimensional variables normalized to the total population, all in lowercase letters):

$$\frac{dc}{dt} = \rho^+ s \cdot i - (\rho^- + \phi)c.$$

Because contacts occur on an hourly or daily basis, which is much faster than timescale of the epidemic, it is sensible to assume  $dc/dt = 0$  and derive an expression for the equilibrium level of associated individuals:

$$\bar{c} = \frac{\rho^+}{\rho^- + \phi} s \cdot i.$$

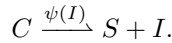
This value of  $\bar{c}$  is intended to represent a dynamic equilibrium at the population level, so it indicates the

average number of contacts per day. With this definition, the transmission rate  $\beta$  introduced in model (1) is:

$$\beta = \phi \frac{\rho^+}{\rho^- + \phi},$$

where  $\phi$  is the probability of infection per contact, and  $\rho^+ / (\rho^- + \phi)$  is the average number of contacts per day, a definition consistent with the literature.<sup>a</sup> The corresponding (non-dimensional) reproduction coefficient can be computed as earlier  $\mathcal{R}_0 = \beta / \gamma$ .

In the presence of infection awareness or policies that discourage or prevent association of individuals, the level of individuals in associated state  $C$  should decrease. A sensible “continuum” approximation of this phenomenon is to model an additional dissociation process that depends on the known infection levels through a *distancing reaction rate parameter*  $\psi(I)$ :



For this to be a well-posed reaction, we require the distancing parameter  $\psi(I)$  to be a non-negative, non-decreasing function of  $I$ , with  $\psi(0) = 0$ . With this model for dissociation, individuals in state  $c$  evolve according to the ODE:

$$\frac{dc}{dt} = \rho^+ s \cdot i - (\rho^- + \phi)c - \psi i \cdot c,$$

which equilibrates to:

$$\bar{c} = \left( \frac{\rho^+}{\rho^- + \phi} \right) \frac{1}{1 + \kappa(i)} s \cdot i, \quad \kappa(i) = \frac{\psi(i)}{\rho^- + \phi}.$$

With this equilibrium value for the average contacts, we derive a time-varying expression for the reproduction number that depends on the infection levels:

$$\mathcal{R}(i) = \mathcal{R}_0 \frac{1}{1 + \kappa(i)}. \quad (8)$$

The *distancing function*  $\kappa(i)$  is in units of /time/individual (or fraction of individuals, the equivalent of “copy number” or molar in chemical reaction networks). Thus  $\mathcal{R}(i)$  is non-dimensional like  $\mathcal{R}_0$ .

Expression (8) is equivalent to Hollinger type II functions in ecology, and Michaelis-Menten/Hill functions in chemical kinetics, and indicates that under a policy in which social distancing depends on average on the infection levels, the reproduction number  $\mathcal{R}(i)$  decreases as the infection numbers raise. One can think about the feedback term  $1/(1 + \kappa(i))$  as a reduction of either

<sup>a</sup>This definition of  $\beta$  can be verified by using the law of mass action to write the ODEs of  $s$  and  $i$ . For example

$$\frac{ds}{dt} = -\rho^+ s \cdot i - \rho^- c,$$

in which  $c$  has to be replaced by its equilibrium value  $\bar{c}$ .

the duration or frequency of infectious contacts (social distancing) or of the likelihood of infection through the use of personal protective equipment, which effectively reduces the level of infectiousness of a contact.

With infection-aware distancing, the non-dimensional FSIR model is:

$$\frac{ds}{d\tau} = -\mathcal{R}_0 \frac{1}{1 + \kappa(i)} si = -\mathcal{R}(i) si \quad (9)$$

$$\frac{di}{d\tau} = \left( \mathcal{R}_0 \frac{1}{1 + \kappa(i)} s - 1 \right) i = (\mathcal{R}(i)s - 1)i \quad (10)$$

For the simple case in which  $\kappa(i) = \kappa i$  (distancing function linearly proportional to infections),  $\mathcal{R}(i)$  decreases monotonically as a function of  $i$ , and it decreases more steeply for large values of  $\kappa$ , as illustrated in Fig. 2. The larger  $\kappa$ , the smaller the value of  $i$  that induces a significant reduction in  $\mathcal{R}_0$  (i.e. “social distancing” occurs in response to a very small known infection level). For example, a value of  $\kappa = 2$  results in  $\mathcal{R}(i) = \mathcal{R}_0/2$  when  $i = 0.5$ ; a value of  $\kappa = 10$  cuts in half  $\mathcal{R}_0$  much sooner, when  $i = 0.1$ .

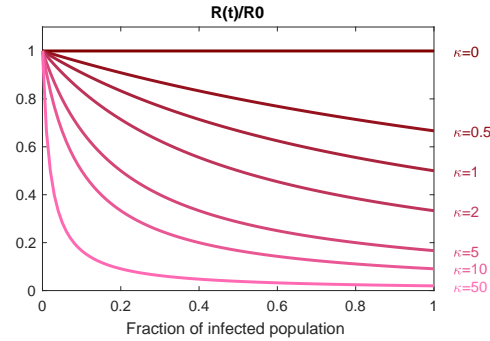


Fig. 2. In the case of distancing function linearly proportional to infections,  $\kappa(i) = \kappa i$ , the infection-dependent reproduction number (8) is monotonically decreasing as a function of infections, for any choice of  $\kappa \geq 0$ .

The distancing function  $\kappa(i)$  models the average population response to knowledge of current infection numbers, in relation to typical interaction patterns; this coefficient could also be used to model the collective “trust” in infection information. For  $\kappa(i) = 0$ , i.e. there is no reaction/policy, nor trust on infection data, then  $\mathcal{R}(i(\tau)) = \mathcal{R}_0$ . (Similarly, if there are no infections and  $i(\tau) = 0$ , then we have no change in  $\mathcal{R}(i(\tau)) = \mathcal{R}_0$  because  $\kappa(0) = 0$ ).

The time varying reproduction number  $\mathcal{R}(i)$  introduces a *negative* feedback loop in the epidemic model, because captures the fact that society decreases interactions in response to an increase of infections, thereby reducing the reproduction number. The model captures also the fact that society is expected to return to typical interaction patterns when infections are not present.

### Structural properties of the fSIR model

*Analysis of equilibria:* Local equilibrium analysis and global stability analysis of SIR models with nonlinear transmission rates has been extensively carried out in the literature [20], [22], [6]; Capasso and Serio demonstrate global positivity, uniqueness, and global stability of the solutions assuming the derivative of the nonlinear transmission rate is bounded and has a maximum at  $i = 0$ . In the case of distancing function linearly proportional to infections ( $\kappa(i) = \kappa i$ ), the fSIR model (9) inherits the equilibrium properties of the original SIR model. If  $i_0 = 0$  ( $r_0 = 0$ ), the system remain at the infection-free equilibrium  $E_0 = (s_0, 0, 0)$  because all derivatives are identically zero. For any  $i_0 > 0$ , the solutions are bounded and evolve in the invariant set  $\mathcal{P} = \{s \leq s_0, i \leq 1, r \leq 1\}$ . If  $\mathcal{R}_0 s_0 \leq 1 + \kappa i_0$ , the infected population is non-increasing because  $di/d\tau \leq 0$ , the epidemic does not start and the system reaches the disease-free equilibrium  $\bar{E} = (\bar{s}, 0, \bar{r})$ . Like in the SIR model, because  $s_0 \leq 1$ , for the epidemic to start it is necessary that  $\mathcal{R}_0 > 1 + \kappa i_0$ .

If  $\mathcal{R}_0 s_0 > 1 + \kappa i_0$ ,  $di/d\tau > 0$  until the susceptible population decreases to the value  $s = s_{crit} = (1 + \kappa i_{max})/\mathcal{R}_0 > \mathcal{R}_0$  at which  $i(\tau) = i_{max}$ . As the susceptible population continues to decrease, so does the infected population and the system reaches the disease-free equilibrium  $E = (\bar{s}, 0, \bar{r})$ .

**Proposition 1** Assume  $\mathcal{R}_0 s_0 > 1 + \kappa i_0$ . The disease-free equilibrium  $E = (\bar{s}, 0, \bar{r})$  is structurally stable.

*Proof* The Jacobian of the fSIR model is:

$$J = \mathcal{R}_0 \begin{bmatrix} -\frac{\bar{i}}{1+\kappa\bar{i}} & -\frac{\bar{s}}{(1+\kappa\bar{i})} \\ \frac{\bar{i}}{1+\kappa\bar{i}} & \frac{\bar{s}}{(1+\kappa\bar{i})^2} - \frac{1}{\mathcal{R}_0} \end{bmatrix}. \quad (11)$$

At the disease-free equilibrium  $E = (\bar{s}, 0, \bar{r})$ ,  $J$  is identical to the Jacobian of the SIR model:

$$J_0 = \begin{bmatrix} 0 & -\bar{s} \\ 0 & \mathcal{R}_0 \bar{s} - 1 \end{bmatrix},$$

which is a structurally stable matrix (at equilibrium  $\mathcal{R}_0 \bar{s} < 1$ ).  $\square$

*Analysis of the solutions:*

**Problem 1** The fSIR model (9) with initial conditions  $s_0, i_0, r_0$  and  $s_0 \mathcal{R}_0 > 1 + \kappa(i_0)$  defines an initial value problem (IVP) with non-negative solutions. We assume the distancing function  $\kappa(i)$  is a non-negative, non-decreasing function with  $\kappa(0) = 0$ , and we look for properties of the solutions of this IVP that hold for any  $\mathcal{R}_0$  and are therefore structural. These properties will be contrasted to the limit case  $\kappa(i) = 0$  that corresponds to the IVP defined by the SIR model (4). The solution

for  $\kappa(i) = 0$  as well as its features will be denoted with the superscript  $^0$  (e.g.  $i(\tau) = i^0(\tau)$  if  $\kappa(i) = 0$ ).

In the general case of a nonlinear distancing function  $\kappa(i)$ , I will show that the peak of infections in the fSIR model is *structurally* smaller than the infection peak for the SIR model, for any non-negative, non-decreasing  $\kappa(i)$ . No assumption is needed on the derivative of  $\kappa(i)$  [6].

**Proposition 2** In Problem 1, for any  $\mathcal{R}_0$  and for any  $\kappa > 0$ , we have:

$$i_{max} < i_{max}^0.$$

*Proof* Following the same approach used to derive (7), the peak of infection for the fSIR model can be estimated from the directional derivative:

$$\frac{di}{ds} = -1 + \frac{1 + \kappa(i)}{\mathcal{R}_0 s}.$$

We then obtain the infinitesimal expression:

$$di = -ds + \frac{ds}{\mathcal{R}_0 s} + \kappa(i) \frac{ds}{\mathcal{R}_0 s}, \quad (12)$$

in which the last term cannot be easily integrated, but it can be replaced by a simpler expression. We note that  $dr = id\tau$ , therefore  $di = -ds - id\tau$ . At the same time we just showed that:

$$di = -ds + \frac{(1 + \kappa(i))}{\mathcal{R}_0} \frac{ds}{s}, \quad (13)$$

which means

$$id\tau = \frac{(1 + \kappa(i))}{\mathcal{R}_0} \frac{ds}{s}.$$

Rearranging terms, we find that

$$\frac{1}{\mathcal{R}_0} \frac{ds}{s} = -\frac{i}{1 + \kappa(i)} d\tau,$$

which can be substituted in the last term of equation (12):

$$di = -ds + \frac{ds}{\mathcal{R}_0 s} - i \frac{\kappa(i)}{1 + \kappa(i)} d\tau,$$

thus we obtain the expression:

$$i(\tau) = s_0 + i_0 - s + \frac{1}{\mathcal{R}_0} \log \frac{s}{s_0} - \int_0^\tau i \frac{\kappa(i)}{1 + \kappa(i)} d\sigma, \quad (14)$$

The infection peak occurs at  $s_{crit} = (1 + \kappa(i_{max}))/\mathcal{R}_0$ , which can be substituted in equation (14):

$$i_{max}(\tau_{max}) = s_0 + i_0 - \frac{1 + \kappa(i_{max})}{\mathcal{R}_0} + \frac{1}{\mathcal{R}_0} \log \left( \frac{1 + \kappa(i_{max})}{\mathcal{R}_0 s_0} \right) - \int_0^{\tau_{max}} i \frac{\kappa(i)}{1 + \kappa(i)} d\sigma. \quad (15)$$

When  $\kappa(i) = 0$  we recover the original SIR infection peak expression (7). The difference between the peak value (15) and the peak when  $\kappa(i) = 0$  ( $i_{max}^0$ ) is:

$$i_{max} - i_{max}^0 = -\frac{1}{\mathcal{R}_0} (\kappa(i_{max}) - \log(1 + \kappa(i_{max}))) - \int_0^{\tau_{max}} i \frac{\kappa(i)}{1 + \kappa(i)} d\sigma.$$

Because  $\log(1+x) < x$  for any  $x > 0$ , and because the last integral is strictly positive, we conclude that  $i_{max} < i_{max}^0$  for any  $\kappa > 0$ .  $\square$

**Corollary 1** *In Problem 1, the solution  $s(\tau)$  is always lower bounded by the solution  $s^0(\tau)$ . In particular the equilibrium satisfies  $\bar{s} > \bar{s}^0$ .*

*Proof* First note that  $ds/d\tau$  is always negative. Then we have that:

$$\frac{ds}{d\tau} = -\mathcal{R}_0 \frac{1}{1 + \kappa(i)} si > -\mathcal{R}_0 s^0 i^0,$$

since the function  $\frac{1}{1 + \kappa(i)}$  is strictly less than one because the distancing function is a non-negative function of  $i$ . Because this inequality holds for arbitrary values of  $i$ , we can invoke the comparison principle [17]:

$$\frac{ds^0}{d\tau} < \frac{ds}{d\tau} \Rightarrow s^0(\tau) < s(\tau).$$

In the limit for  $\tau \rightarrow \infty$ , the steady state values satisfy  $\bar{s} > \bar{s}^0$ .  $\square$

This proposition shows that, relative to an epidemic that lacks negative feedback, the fSIR model structurally settles to a larger susceptible population in the disease-free equilibrium. As a consequence, the equilibrium recovered population satisfies  $\bar{r} < \bar{r}^0$ .

In the case of distancing function linearly proportional to infections, the fSIR model can be solved exactly in phase space following the steps in [6] and [1]. Starting from the directional derivative,

$$\frac{di}{ds} = -1 + \frac{1 + \kappa i}{\mathcal{R}_0 s},$$

terms can be rearranged to find an ordinary differential equation for  $i(s)$ :

$$s \frac{di}{ds} - \frac{\kappa}{\mathcal{R}_0} i(s) = -s + \frac{1}{\mathcal{R}_0}.$$

With the change of variable  $z = \ln(s)$ , we find:

$$\frac{di(z)}{dz} - \frac{\kappa}{\mathcal{R}_0} i(z) = -e^{-z} + \frac{1}{\mathcal{R}_0},$$

which can be solved finding the phase-space expression:

$$i(s) = \left( i_0 + \frac{1}{\kappa} + \frac{\mathcal{R}_0}{\mathcal{R}_0 - \kappa} \right) s^{\frac{\kappa}{\mathcal{R}_0}} - \frac{1}{\kappa} - \frac{\mathcal{R}_0}{\mathcal{R}_0 - \kappa} s. \quad (16)$$

In the particular case when  $\kappa = \mathcal{R}_0$ , the solution is  $i(s) = (s-1)/\mathcal{R}_0 - s \ln s$ . By setting  $i(s) = 0$  one can find the final size of the susceptible population. By substituting  $i_{max} = \frac{\mathcal{R}_0 s_{crit} - 1}{\kappa}$  in equation (16), one can derive  $s_{crit}$ :

$$s_{crit} = \frac{1}{\mathcal{R}_0} \left( i_0 \kappa (\mathcal{R}_0 - \kappa) + 1 + \kappa - \frac{\kappa}{\mathcal{R}_0} \right)^{\frac{1}{1 - \frac{\kappa}{\mathcal{R}_0}}}$$

and the corresponding infection peak can be found exactly; it can be verified that the infection peak always decreases with  $\kappa$  as predicted by Proposition 2.

Next, continuing to focus on the case in which the distancing function is linearly proportional to infections,  $\kappa(i) = \kappa i$ , we report two additional structural results for Problem 1.

**Corollary 2** *In Problem 1 with  $\kappa(i) = \kappa i$ , the solution  $i(\tau)$  is upper bounded by the solution  $i^0(\tau)$  for  $0 < \tau < \tau_{max}^0$ , where  $\tau_{max}^0$  is the time at which the maximum  $i_{max}^0$  occurs.*

*Proof* For  $0 < \tau < \tau_{max}$  we know that  $di/d\tau > 0$ , so  $i(\tau)$  is monotonically increasing for any value of  $\kappa$  including  $\kappa = 0$ . Due to Proposition 2,  $i_{max} < i_{max}^0$  for any value of  $\kappa > 0$ . Due to monotonicity of the solutions, it must be that  $i(\tau) < i^0(\tau)$  for all  $0 < \tau < \min(\tau_{max}, \tau_{max}^0)$ . Because Proposition 3 shows that  $\tau_{max}^0 < \tau_{max}$  for all  $\kappa > 0$ , we conclude that  $i(\tau) < i^0(\tau)$  for all  $0 < \tau < \tau_{max}^0$ .  $\square$

**Corollary 3** *In Problem 1 with linear distancing function  $\kappa(i) = \kappa i$ , the time  $\tau_{max}$  at which the peak of infection occurs is always larger than the peak time  $\tau_{max}^0$  corresponding to  $\kappa = 0$ :*

$$\tau_{max} > \tau_{max}^0. \quad (17)$$

*Proof* We show that  $d\tau_{max}/d\kappa > 0$  for any  $\kappa > 0$ , which means that the peak time can only increase as  $\kappa$  increases. First, recall that  $s(\tau_{max}) = s_{crit} = (1 + \kappa i_{max})/\mathcal{R}_0$ . Then:

$$\frac{ds(\tau)}{d\kappa} \Big|_{\tau=\tau_{max}} = \frac{\kappa}{\mathcal{R}_0} \frac{di_{max}}{d\kappa}$$

Using the chain rule  $ds/d\kappa = (ds/d\tau)(d\tau/d\kappa)$ . At  $\tau = \tau_{max}$ ,  $ds/d\tau = -i_{max}$ , therefore:

$$\frac{d\tau_{max}}{d\kappa} = -\frac{\kappa}{i_{max} \mathcal{R}_0} \frac{di_{max}}{d\kappa}$$

From Proposition 2, we know that  $di_{max}/d\kappa < 0$  and we conclude that  $d\tau_{max}/d\kappa > 0$ .  $\square$

We conclude with a qualitative observation on the fSIR solution (Problem 1) with distancing function

$\kappa(i) = \kappa i$ , when  $\kappa$  is very large, thus  $\kappa i \gg 1$ . In this case, the fSIR can be approximated by the linear system:

$$\frac{d\hat{s}}{d\tau} \approx -\frac{\mathcal{R}_0}{\kappa} \hat{s}, \quad \frac{d\hat{i}}{d\tau} \approx \frac{\mathcal{R}_0}{\kappa} \hat{s} - \hat{i}. \quad (18)$$

The solution  $\hat{i}(\tau)$  can be found exactly:

$$\hat{i}(\tau) = i_0 e^{-\tau} + s_0 \frac{\mathcal{R}_0}{\kappa - \mathcal{R}_0} \left( e^{-\tau} - e^{-\frac{\mathcal{R}_0}{\kappa} \tau} \right).$$

This approximation shows that if  $\mathcal{R}_0/\kappa \ll 1$  the infection dynamics converge very slowly to the disease free equilibrium  $\hat{i} = 0$  (convergence is dominated by the constant  $\mathcal{R}_0/\kappa$ ).

#### Numerical simulations

For simplicity and illustrative purposes, in these numerical simulations I consider the fSIR model with linear infection awareness  $\kappa(i) = \kappa i$ .

*Infection-aware distancing reduces the peak of infection and does not postpone the peak significantly:* Fig. 3, top, shows the numerically integrated solution of the fSIR model (9) with  $\mathcal{R}_0 = 2.5$  as the parameter  $\kappa$  is varied. ( $\mathcal{R}_0 = 2.5$  corresponds to a choice of  $\beta = 0.25$  and  $\gamma = 1/10$ , i.e. the average time to recovery or death assumed to be 10 days; for comparison, the estimated average time to recovery in the COVID-19 epidemic is about 17 days for hospitalized patients [27]). These simulations confirm that the peak of infections decreases with a large  $\kappa$ , relative to the case  $\kappa = 0$  (SIR without feedback). Fig. 3, bottom, shows the temporal evolution of the reproduction number in each simulation in the top panel: when infections increase,  $\mathcal{R}(\tau)$  decreases and adjusts to the nominal level ( $\mathcal{R}_0 = 2.5$ ) when infections are not present. These simulations also confirm the results of Propositions 2, and 3, as the infection peak is always reduced and delayed: Fig. 4 shows that a feedback parameter  $\kappa = 2$  (taken as an illustrative example) the infection peak size can be reduced by about 30%, but this also causes a 30% extension of the time during which more than 2.5% of the population is infected.

*Effects of delayed infection awareness:* With simulations I examine whether a delay  $\Delta$  in obtaining infection information can compromise the effects of feedback. A delay is included in the transmission rate expression:

$$\frac{ds}{d\tau} = -\mathcal{R}(i)si, \quad \mathcal{R}(i) = \mathcal{R}_0 \frac{1}{1 + \kappa i(\tau - \Delta)}, \quad (19)$$

$$\frac{di}{d\tau} = (\mathcal{R}(i)s - 1)i. \quad (20)$$

Global stability analysis of SIR models with nonlinear transmission and delays have been demonstrated in [15], and likely apply to this model.

For illustrative purposes, I choose a feedback parameter  $\kappa = 2$  that remains fixed in these simulations, with

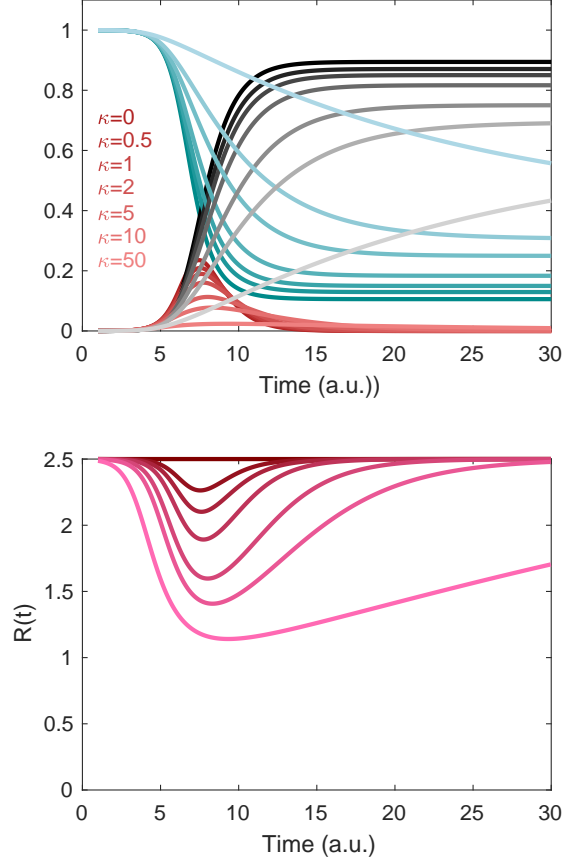


Fig. 3. Numerically integrated solutions of the fSIR model. Top: Susceptible (green), infected (red), and recovered (gray) individuals when the parameter  $\kappa$  is varied (low to high, color shades from dark to light). Bottom: Evolution of the reproduction number in time computed from the simulations above; this can be interpreted as a qualitative measure of the implemented social distancing policies.

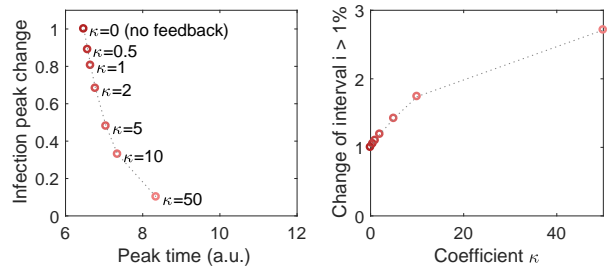


Fig. 4. Left: Peak time versus peak value of infections for different values of the feedback parameter  $\kappa$ . This plot evidences that the peak is not delayed as in models where the transmission rate is constant and low. Right: The duration of infections is longer in the presence of feedback; here it is measured as the time interval for which the fraction of infected individuals is larger than 2.5% of the population.



$\mathcal{R}_0 = 2.5$  ( $\beta = 0.25$  and  $\gamma = 1/10$ ). Fig. 5 shows that a delay of up to 7 days increases the peak by less than 10%, but a 14 day delay causes a 25% increase in the peak, offsetting the peak reduction obtained by introducing feedback (the simulated non-dimensional delay is divided by the rescaling constant  $\gamma = 1/10$ ).

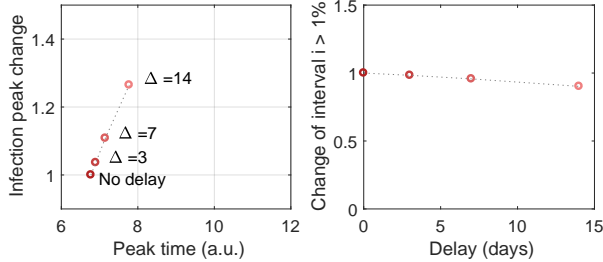


Fig. 5. Effects of delays on the peak size and duration. Left: Change in peak size in the presence of delays, relative to the case in which feedback is present without delay and  $\kappa = 2$ . Right: The amount of time for which the fraction of infected population exceeds 2.5% is slightly reduced when delays are between 0 and 14 days.

*The fSIR model captures current COVID-19 infection trends:* The fSIR model was fitted to COVID-19 temporal series data for infections, recoveries, and deaths available from the Johns Hopkins Github repository [9]. I selected data from six western democracies (Italy, France, UK, Spain, Germany and the US) with comparable infection and recovery reporting patterns. In addition, in these countries strict social distancing measures were not *immediately* enforced during the early stages of the epidemic, thus it is reasonable to use a compartment model. Further, the reported infections and deaths in these countries have a similar doubling time of 2-4 days in the early (exponential) stages [2]. Finally infection, recovery, and deaths reports are unlikely to have been systematically manipulated, although there are substantial differences in the protocols for infection and post-mortem testing. Because all these countries enforced social distancing measures at different times during the local evolution of the pandemic, the fSIR model should capture these differences in the fitted parameter  $\kappa$ . Yet, we should keep in mind that the population of infected individuals is largely underestimated (worldwide) due to lack of testing resources.

Fitting results are in Fig. 6. The data were processed to compute active infections in a given day, and recoveries and deaths were summed and consolidated into the “recovered” compartment. All data were normalized by country population and thresholded to include only data collected after infections exceed two per million. Parameters were fitted with constraints  $\beta \in [0 \ 0.6]$ ,  $\gamma \in [1/17 \ 1/10]$ , and  $\kappa \in [0 \ 10 \cdot 10^3]$ ; in the fitting score function, the infection prediction error was assigned a 100-fold penalty relative to the recovery

data, with the expectation that recoveries may not be accurately reported for non-hospitalized patients; as a consequence, the fitted model reproduces infection data much more closely than recovery data. (An SIR model fits the same data very poorly, as it unrealistically assumes a constant transmission rate  $\beta$ .)

If the fSIR model is fitted to data scaled by X-fold (*i.e.* infections and recoveries are believed to be X-times larger than reported), the fitted  $\kappa$  qualitatively scales by a factor  $1/X$ , while changes in fitted  $\beta$  and  $\gamma$  are negligible.

The fitted value of  $\kappa$  can be interpreted as the inverse of the infections observed when the reproduction number is half its initial value. Thus, low fitted values of  $\kappa$  indicate that a country enacted infection-dependent social distancing late in the epidemic (higher infection numbers). Unsurprisingly, among the countries considered here the highest  $\kappa$  is fitted for Germany, and the lowest for the UK and the US. The fact that overall the model fits poorly infection data from Germany points to the fact that their management of  $\mathcal{R}(t)$  may not be based on mere infection numbers, and may have been substantially different from other countries from the very initial stages, resulting in lower infection levels and lower mortality.

The data fitting reported here has largely an illustrative purpose, and is not meant to make predictions. However, from this exercise it is clear that a protocol of social distancing based on infection awareness (enforce distancing when infections are high, relax distancing when infections decrease) does reduce the peak of infections, but it can also considerably lengthen the duration of the epidemic as shown by the linear approximation (18) and by simulations in Fig. 5. With this in mind, in Fig. 7 we show a projection of infections for Spain and Italy based on the fitted fSIR parameters. Although the peak of infections appears near, infection numbers may remain roughly constant for years to come, consistently with the observations made on the fSIR linear approximation (18). The computed reproduction number remains very close or slightly above one throughout the projected simulation. This may be or may not be a reasonable societal target, depending on considerations that balance the sustainability of a long-term lockdown with the emergence of therapeutic advances and vaccines that may reduce mortality rates and improve recovery time, making it possible for a healthcare system to absorb a bounded number of infections. Similar predictions highlighting the pitfalls of relaxing social distancing are put forward by many models that are more complex and accurate than the one presented here [19], [11].



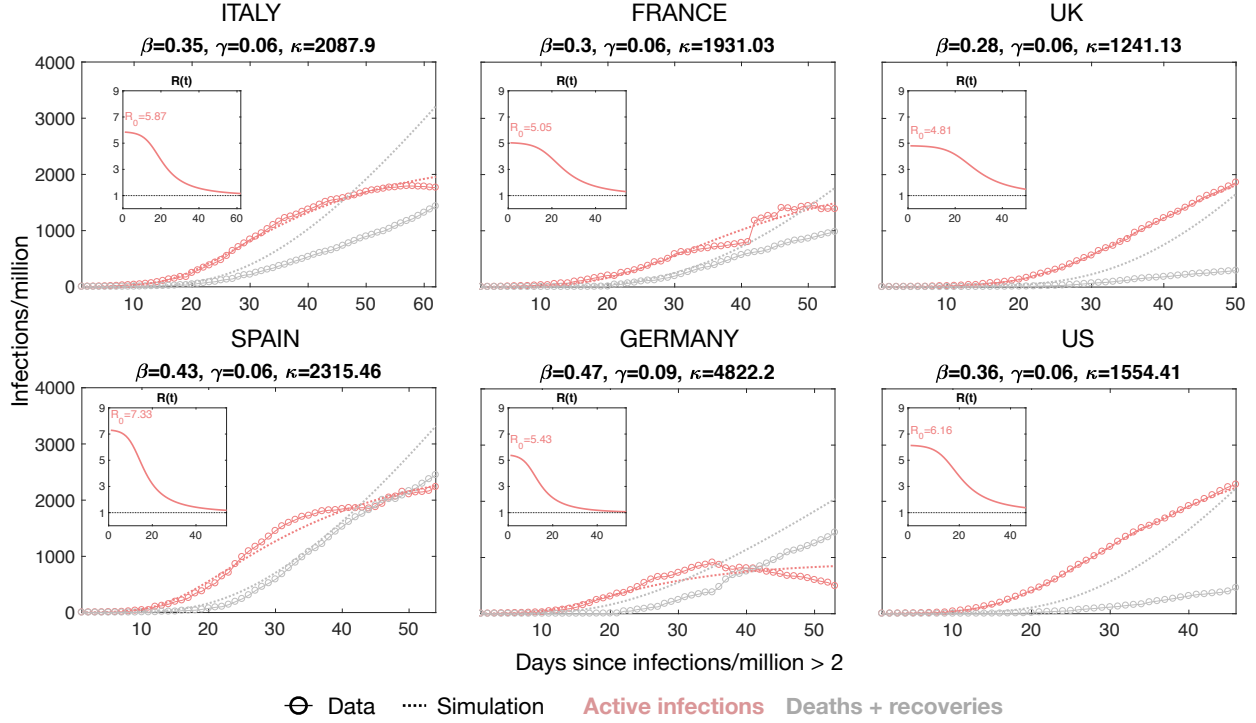


Fig. 6. The fSIR model parameters  $\beta$ ,  $\gamma$ , and  $\kappa$  were fitted to COVID-19 data of active infections as well as recoveries and deaths for six different countries up to April 25, 2020. Data were obtained from the JHU Github repository [9]. A 100-fold fitting penalty was assigned to infection data relative to recoveries. The model captures well most infection data with the exception of Germany, which presents the highest fitted  $\kappa$  indicating a stronger distancing in relation to infection information. Results are discussed in Section -B.

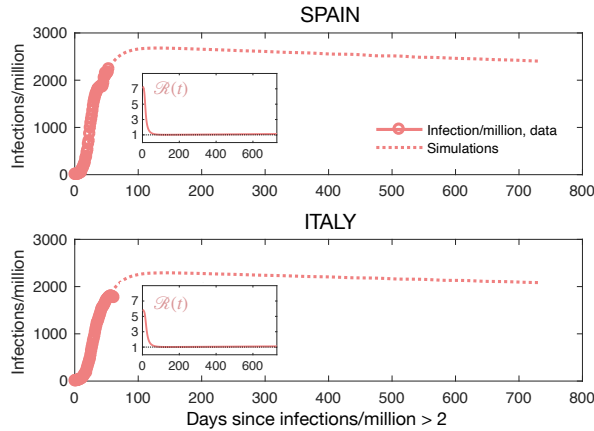


Fig. 7. Theoretical projection of infection data using the fitted fSIR model for Spain (top) and Italy (bottom); inlet shows predicted  $\mathcal{R}(t)$ . This simulation is not meant to provide accurate predictions, rather to illustrate the concept that feedback based purely on infection-aware distancing may significantly extend the epidemic according to the very simple model presented here. Adjustments of the coefficient  $\kappa$  may overcome this problem.

## CONCLUSION AND DISCUSSION

I have derived and analysis of a modified SIR model, here named feedback SIR (fSIR), in which infection-based distancing introduces a reproduction

number that decreases a continuous function of infection levels, generating a negative feedback loop. The model is derived from first principles assuming a well-mixed population and assuming individuals reduce their contacts the more infections are reported, and using a standard time-scale separation argument the transmission rate function takes the form of a Hollinger type II or Hill function that are widely adopted in ecology, chemistry and biology. In the special case of a distancing function that is linear with respect to infection information, this model requires only one additional parameter to capture the effects of social distancing, and illustrates the tradeoffs between reducing the infection peak while maintaining a short epidemic course.

## METHODS

Differential equations were integrated with a forward Euler method in MATLAB using custom scripts, or using MATLAB's `ode45`. Data fitting was done using MATLAB's `fmincon`.

## REFERENCES

- [1] Rose Baker. Reactive social distancing in a SIR model of epidemics such as COVID-19. *arXiv preprint arXiv:2003.08285*, 2020.

- [2] Andrea L Bertozzi, Elisa Franco, George Mohler, Martin B Short, and Daniel Sledge. The challenges of modeling and forecasting the spread of COVID-19. *arXiv preprint arXiv:2004.04741*, 2020.
- [3] Michelangelo Bin, Peter Cheung, Emanuele Crisostomi, Pietro Ferraro, Connor Myant, Thomas Parisini, and Robert Shorten. On fast multi-shot epidemic interventions for post lock-down mitigation: Implications for simple covid-19 models. *arXiv preprint arXiv:2003.09930*, 2020.
- [4] Martin CJ Bootsma and Neil M Ferguson. The effect of public health measures on the 1918 influenza pandemic in US cities. *Proceedings of the National Academy of Sciences*, 104(18):7588–7593, 2007.
- [5] Bruno Buonomo, Alberto d’Onofrio, and Deborah Lacitignola. Global stability of an SIR epidemic model with information dependent vaccination. *Mathematical biosciences*, 216(1):9–16, 2008.
- [6] Vincenzo Capasso and Gabriella Serio. A generalization of the Kermack-McKendrick deterministic epidemic model. *Mathematical Biosciences*, 42(1-2):43–61, 1978.
- [7] Francesco Casella. Can the COVID-19 epidemic be managed on the basis of daily data? *arXiv preprint arXiv:2003.06967*, 2020.
- [8] Ensheng Dong, Hongru Du, and Lauren Gardner. An interactive web-based dashboard to track COVID-19 in real time. *The Lancet*, 2020. <https://plague.com/>.
- [9] Ensheng Dong, Hongru Du, and Lauren Gardner. An interactive web-based dashboard to track COVID-19 in real time. *The Lancet infectious diseases*, 2020.
- [10] Sebastian Funk, Erez Gilad, Chris Watkins, and Vincent AA Jansen. The spread of awareness and its impact on epidemic outbreaks. *Proceedings of the National Academy of Sciences*, 106(16):6872–6877, 2009.
- [11] Giulia Giordano, Franco Blanchini, Raffaele Bruno, Patrizio Colaneri, Alessandro Di Filippo, Angela Di Matteo, and Marta Colaneri. Modelling the COVID-19 epidemic and implementation of population-wide interventions in Italy. *Nature Medicine*, pages 1–6, 2020.
- [12] David Greenhalgh, Sourav Rana, Sudip Samanta, Tridip Sardar, Sabyasachi Bhattacharya, and Joydev Chattopadhyay. Awareness programs control infectious disease—multiple delay induced mathematical model. *Applied Mathematics and Computation*, 251:539–563, 2015.
- [13] Tiberiu Harko, Francisco S. N. Lobo, and M. K. Mak. Exact analytical solutions of the susceptible-infected-recovered (SIR) epidemic model and of the SIR model with equal death and birth rates. *Applied Mathematics and Computation*, 236:184–194, 2014.
- [14] Herbert W Hethcote. Qualitative analyses of communicable disease models. *Mathematical Biosciences*, 28(3-4):335–356, 1976.
- [15] Gang Huang, Yasuhiro Takeuchi, Wanbiao Ma, and Daijun Wei. Global stability for delay SIR and SEIR epidemic models with nonlinear incidence rate. *Bulletin of mathematical biology*, 72(5):1192–1207, 2010.
- [16] William Ogilvy Kermack and Anderson G McKendrick. A contribution to the mathematical theory of epidemics. *Proceedings of the royal society of London. Series A, Containing papers of a mathematical and physical character*, 115(772):700–721, 1927.
- [17] H. K. Khalil. *Nonlinear Systems*. Prentice Hall, 2002.
- [18] Istvan Z Kiss, Jackie Cassell, Mario Recker, and Péter L Simon. The impact of information transmission on epidemic outbreaks. *Mathematical biosciences*, 225(1):1–10, 2010.
- [19] Stephen M Kissler, Christine Tedijanto, Edward Goldstein, Yonatan H Grad, and Marc Lipsitch. Projecting the transmission dynamics of SARS-CoV-2 through the postpandemic period. *Science*, 2020.
- [20] Andrei Korobeinikov and Philip K Maini. Non-linear incidence and stability of infectious disease models. *Mathematical medicine and biology: a journal of the IMA*, 22(2):113–128, 2005.
- [21] Adam J Kucharski, Timothy W Russell, Charlie Diamond, Yang Liu, John Edmunds, Sebastian Funk, and Rosalind M Eggo. Early dynamics of transmission and control of covid-19: a mathematical modelling study. *The Lancet, Infectious Diseases*, 2020. March 11, 2020.
- [22] Wei-min Liu, Herbert W Hethcote, and Simon A Levin. Dynamical behavior of epidemiological models with nonlinear incidence rates. *Journal of mathematical biology*, 25(4):359–380, 1987.
- [23] Bastian Prasse, Massimo A. Achterberg, Long Ma, and Piet Van Mieghem. Network-based prediction of the 2019-ncov epidemic outbreak in the Chinese province Hubei, 2020. <https://arxiv.org/pdf/2002.04482.pdf>.
- [24] Umberto Rosini. COVID-19 Italia - Monitoraggio situazione, 2020. GitHub repository of data from Italy COVID-19 epidemic <https://github.com/pcm-dpc/COVID-19>.
- [25] Sudip Samanta and Joydev Chattopadhyay. Effect of awareness program in disease outbreak—a slow-fast dynamics. *Applied Mathematics and Computation*, 237:98–109, 2014.
- [26] Duo Yu, Qianying Lin, Alice PY Chiu, and Daihai He. Effects of reactive social distancing on the 1918 influenza pandemic. *PLoS one*, 12(7), 2017.
- [27] Fei Zhou, Ting Yu, Ronghui Du, Guohui Fan, Ying Liu, Zhibo Liu, Jie Xiang, Yeming Wang, Bin Song, Xiaoying Gu, et al. Clinical course and risk factors for mortality of adult inpatients with covid-19 in Wuhan, China: a retrospective cohort study. *The Lancet*, 2020.